Eurasian J. Sci. Eng., 2023, 9(3), 154-165
https://doi.org/10.23918/eajse.v9i3p14

Published by Tishk International University
Available at: https://eajse.tiu.edu.iq/submit/

RESEARCH ARTICLE
Open Access

Assessing The Impact Of Urbanization On Flood Hazards In Ranya City, Using GIS And Remote Sensing

Kaifi Chomani[1]*

[1] Civil Engineering Department, University of Raparin, Ranya, Sulaymaniyah, Kurdistan Region 46012, Iraq.

Article History
Received: 13.06.2023
Revised: 15.01.2024
Accepted: 17.01.2024
Published: 21.01.2024
Communicated by: Prof. Bayan Salim
**Email address:*
kaifi.chomani@uor.edu.krd
**Corresponding Author*

Copyright: © 2023 by the author. Licensee Tishk International University, Erbil, Iraq. This article is an open access article distributed under the terms and conditions of the Creative Commons Attribution-Noncommercial 2.0 Generic License (CC BY-NC 2.0) https://creativecommons.org/licenses/by-nc/2.0/

Abstract:
Flooding is a major threat to people and the environment all over the world. Ranya city has experienced an increase in flooding as a result of demographic shifts, variations in land use land cover (LULC), and urban development. The objective of this research is to assess the effects of urban growth on flooding in Ranya over a 23-year period. The nine factors used to evaluate flood risk maps were elevation, rainfall, topographic wetness index (TWI), stream power index (SPI), LULC, slope, aspect, drainage density, and distance to roads. Flood hazard and LULC maps were created and analysed using The Analytic Hierarchy Process (AHP), geographic information system (GIS), and satellite remote sensing data for the years 2000 and 2023. The result revealed from 2000 to 2023, the settlement and agricultural area increased by approximately 25 and 9.6%, respectively, while barren land decreased by 34.8%. The 0.09% annual growth in the built-up area was a major factor in the expansion of Ranya's high flood-risk areas. Low, moderate, high, and very high categories were used to define the flood risk areas in Ranya. In zones with a very high flood risk, the extent of the flood hazard area in 2023 increased by 1.9% compared to 2000, while it decreased by 11.4% in zones with a low flood risk. Urban areas, and especially city centres, are significantly more likely to experience flooding. Ranya has seen an enormous increase in the amount of flood-prone areas in the last 23 years due to the city's urbanisation. This study used AHP technique that enables researchers to efficiently monitor the urban environment, which may then be used to substantially reduce damages in Ranya City's flood-prone zones. It also assists decision-makers and state officials in understanding how urban growth affects the environment.

Keywords: *Flood Hazard; GIS; Urbanization; AHP; Remote Sensing; Ranya.*

1. Introduction

Flooding causes major damage around the globe to people's houses, the environment, the economy, human activities, crops, biodiversity, buildings, public transit, and transferring toxic waste [1-6]. Flood damage has been rising despite major improvements in the detection and prevention of floods, and this trends may continue as flood-prone regions become more urbanized [7, 8]. Flooding accounted for 49% of all catastrophe events in 2019 and was the most hazardous type of natural threat [9, 10], and around a million people were killed by floods in the twentieth century [11]. The flooding had both environmental and manmade causes [5], but human interference with the environment can lead to more floods [12-15], resulting in tragic deaths and economic damages [16, 17]. Urban flooding is a leading cause of natural disaster casualties and property loss [18]. Changes in LULC, demographic change, poor governance, food insecurity, rural-to-urban migration, industrialization, and climatological conditions, along with significant rainfall events, all increase the risk of flooding [17, 19-23]. Flooding is a result of changes in hydrological factors caused by urbanisation [24-26]. Sudden shifts in LULC and urbanisation typically increase the risk of flooding [27, 24], which can result in fatalities as well as significant damage to buildings [18]. The study of land-use transitions is significant due to its profound impact on urban hydrological processes [28].

Iraq is particularly at high risk for flooding [29, 30]. Consequently, it has become crucial to identify the dangers, vulnerabilities, and risks related to flooding [31]. To predict flood risks and improve planning and preparation, it is important to find out and measure how changes in land use influence stream flow [32, 33]. To reduce the amount of damage that caused by floods, flood control systems are strictly necessary [18, 34]. Safe and effective precautions are needed to reduce urban flooding resulting from changes in land use [18]. Improved flood risk assessments are achievable through the aid of GIS and remote sensing [35, 36]. A few of the phases of sufficient flood risk management and prevention include the creation of a vulnerability map [37, 38].

Despite the availability of a variety of approaches to assess the flood risk [39, 40], each has both benefits and drawbacks [41]. Furthermore, because underdeveloped countries have limited data availability [42], the usage of publicly available remotely sensed datasets in a GIS system has become increasingly common [5]. Technological developments have enabled the use of satellite data for the accurate forecast of areas vulnerable to floods [7], which can be achieved by integrating flood vulnerability modelling with GIS and satellite remote sensing data [43, 44]. Several research have been carried out to examine the effect of LULC on flooding. [24, 26, 45, 46] assessed how urban growth affected flooding. Sissakian [47] and Askar [48] used a number of methods to analyse the flood risk in the northern parts of Iraq. The flood prone areas in this study were created using the analytical hierarchy process (AHP) and GIS tools. The combination of GIS and multi-criteria decision making (MCDM) is successfully being used to solve problems in a wide range of fields [22, 23, 49-51], including flood risk assessment [52-58]. The merging of AHP with GIS is the most extensively utilized approach to creating flood hazard maps [59]. The AHP approach to evaluating flood damages is economical and time-efficient [56, 60-64].

The reason Ranya City is the subject of this study is that it has experienced significant flooding recently. Ranya, like many other cities in Iraq's Kurdistan Region, has experienced floods in the past, especially during the winter months. Rainstorms recently caused flash floods in several areas of Ranya, including the city centre and nearby villages. The floods damaged main streets, bridges, infrastructure, and crops, and some homes were partially or completely submerged [65, 66]. Only in Raparin's independent administration in 2018, floods caused over a million USD in damage; 415 families were affected, and 9 houses were completely destroyed [65, 67-69]. In addition to disrupting school, the rain's landslides near and on roads made travel between cities impossible [70]. Government entities and decision-makers can use the hazard analysis method outlined in this research, along with its results for flood hazard zones in Ranya, as a guide to improve emergency preparedness and strategic planning.

2. Methods

2.1 Study Area

Ranya is a city located in the Kurdistan Region of Iraq. It is situated in the southeastern part of the region, about 124 kilometres east of the capital city of Erbil. Ranya is the second-largest city in the Sulaymaniyah Governorate, after the city of Sulaymaniyah. Ranya is located at 36° 15' 15" north and 44° 52' 57" east (Fig. 1). New housing complexes, shopping malls, and other infrastructure projects have contributed to Ranya's rapid expansion in recent years. In addition to being home to the University of Raparin, the city also features a number of secondary educational facilities. The rapid urbanisation and development of Ranya can be contributed to the city's transition to autonomous administration from the Sulaymaniyah Governorate in 2012. It is nearly 695 metres above mean sea level and has an area of nearly 27 km2. It has 753 millimetres of precipitation per year [71]. Ranya is situated in a mountainous region and is known for its natural beauty. The city is bounded by beautiful mountains, and the tourist areas of Dokan Lake, Plingan, Qurago, and Sarashkawtan are all nearby. It is also well-known for its farming, particularly for its fruit and vegetable crops. The pressure that population growth is placing on limited resources like land in urban centres is increasing as more people leave rural areas. There isn't much room for the city to expand horizontally and accommodate more people because there are lakes and mountains all around Ranya.

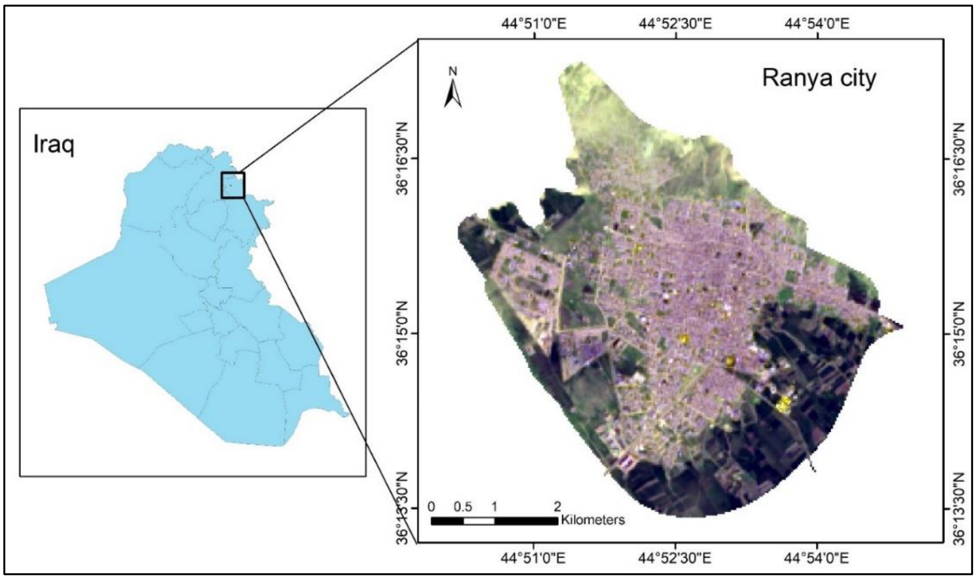

Figure 1: Study area (Ranya city).

2.2 Data and Flood Vulnerability Factors

There are different factors that have relevant combination to flood hazards. The main and secondary factors were defined in this research which had the significant influence on flooding events in the Ranya city. Precipitation, drainage density, elevation, and slope were considered as the main criteria which had the significant effect on the hydrological processes in the city. Moreover, parameters like LULC, aspect, SPI, TWI, and distance to roads were assigned as the secondary factors which have the impact on the flood hazards in Ranya city. For this study, a digital elevation model (DEM) and Landsat OLI images from 2000 and 2023 were acquired from the United States Geological Survey website [27]. The spatial resolution of the OLI/TIRS data bands was 30 m. Data on annual rainfall for the years 1998–2021 were gathered from earlier studies [71, 72].

Elevation, topographic wetness index (TWI), drainage density, rainfall, land use and land cover (LULC), slope, aspect, distance to roads, and stream power index (SPI) were the nine factors (Fig. 2) that were used to evaluate flood risk maps (Fig. 3). We also intended to include soil and geology as parameters, but we decided not to include them because there is only one type of soil and geology in the study and these variables had no significant impact on the research results. Using a pairwise comparison matrix [73-75] and information from expert consultants, we mapped flood susceptibility for the years 2000 and 2023 using the AHP method from the MCDM technique (Table 2). The Analytic Hierarchy Process (AHP) is one of the common used methods of decision-making which offers effective solutions for complex problems by considering multiple criteria.

The method assigns weights to different factors based on their influence. The pairwise compression determines the weights and compares each criteria to others. The AHP calculates the relative importance of the factors which will help in decision making process [49]. Using ArcGIS 10.8 software [76], thematic layers, flood-prone maps, LULC classifications, the AHP method, a weighted overlay (Table 3), and a result analysis were carried out. Fig. 4 shows a detailed illustration of the study's methodology. Rainfall map were created from the collected data and distance to roads were generated from digitizing the roads from satellite images between 2000 and 2023 using ArcGIS 10.8 software. Elevation, TWI (Eq. 1), SPI (Eq. 2), slope, aspect, and drainage density maps are extract from DEM data. With the help of ISO cluster unsupervised classification, LULC maps with three classes were produced for the years 2000 and 2023. Using the Kappa coefficient and Google Earth Pro, the LULC classification's accuracy was assessed for the years 2000 and 2023 with a total of 100 random points, obtaining accurate results of 88% and 91%, respectively.

(1) $$TWI = ln(\frac{As}{tan(slope)})$$

Where the slope is represented in degrees, TWI = the topographic wetness index, and As = the catchment area (m2 m1) [5].

(2) $$SPI = A_s * tan\beta$$

Where SPI represents the stream power index, A_s = basin area in (m2), and β = the slope (in degrees) [77].

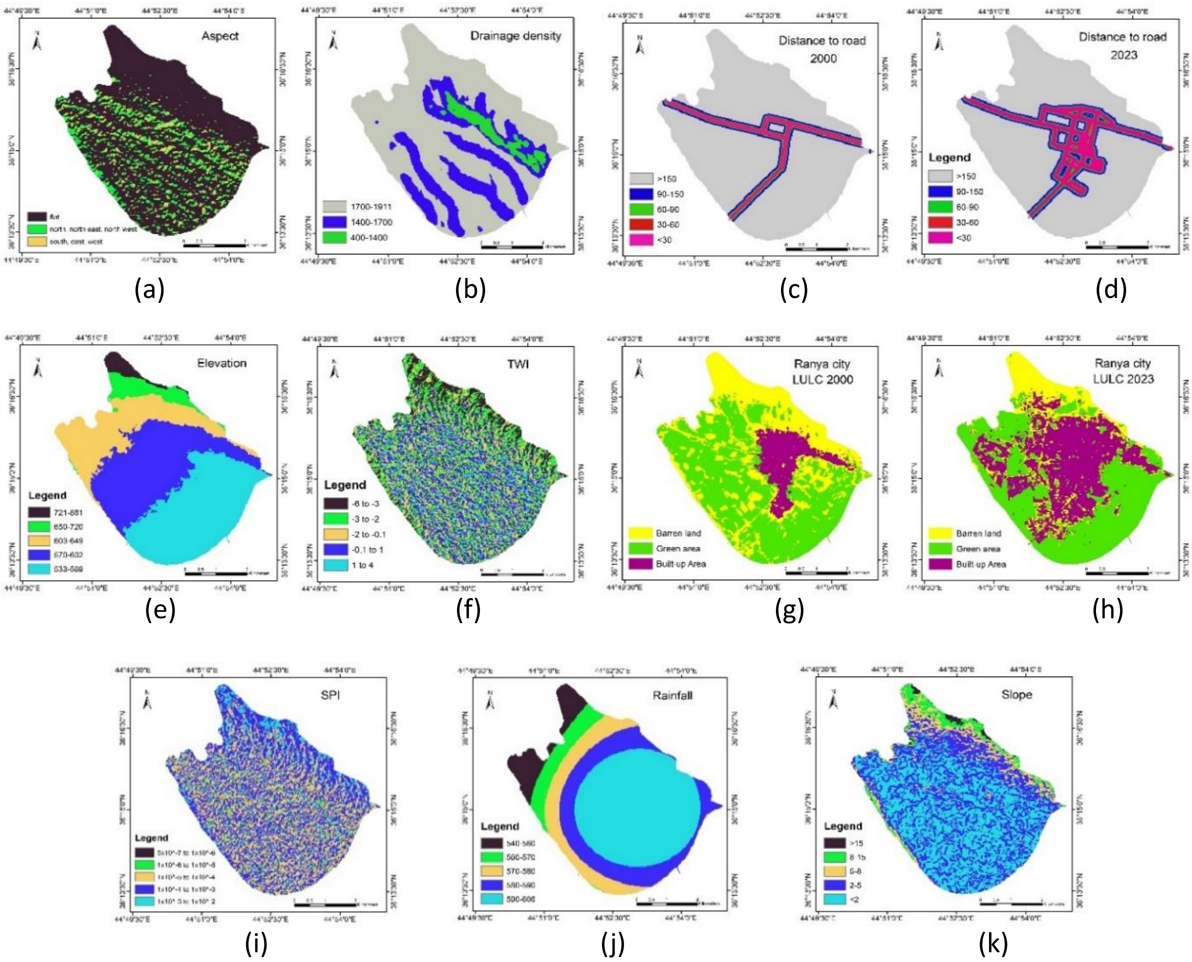

Figure 2: Flood hazard factors used in AHP method: (a) aspect, (b) drainage density, (c) distance to road 2000, (d) distance to road 2023, (e) elevation, (f) TWI, (g) Ranya LULC 2000, (h) Ranya LULC 2023, (i) SPI, (j) rainfall, (k) slope.

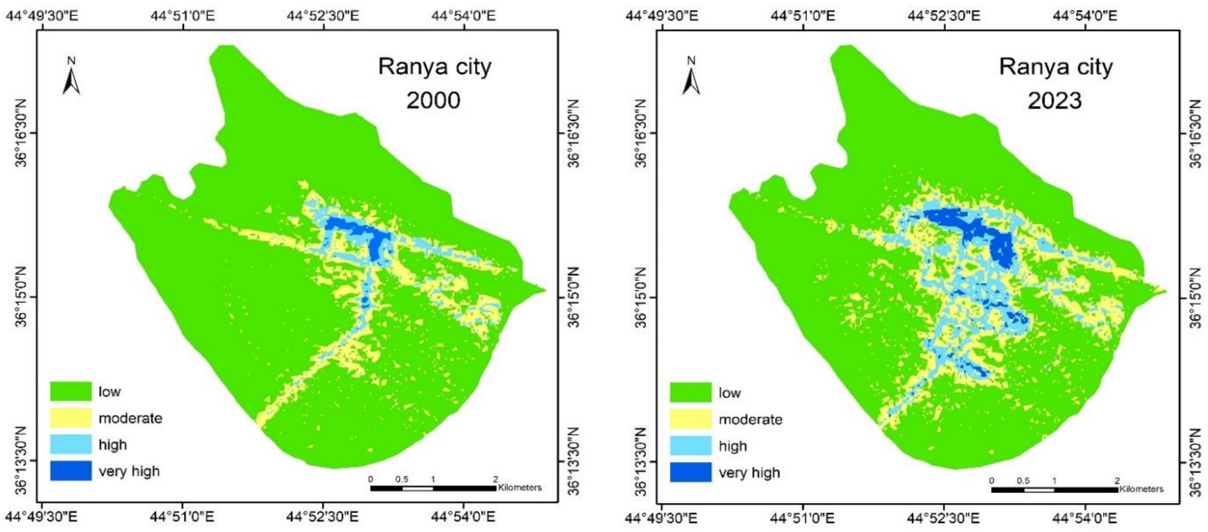

(a) (b)

Figure 3: Flood risk areas in Ranya: (a) 2000, (b) 2023.

3. Results and Discussions:

3.1 Change in LULC

The LULC classification results demonstrate an enormous expansion in urban areas as well as a transition in Land use patterns. Over a 23-year period, there were approximately 25% and 9.6% increases in settlement features and agriculture, respectively, and a 34.8% reduction in the barren land (Table 1). The growth rate in Land use and land cover is calculated between 2000 and 2023. The annual growth rate in the residential area was 1.09%, demonstrating significant urban growth in Ranya during the last twenty-three years.

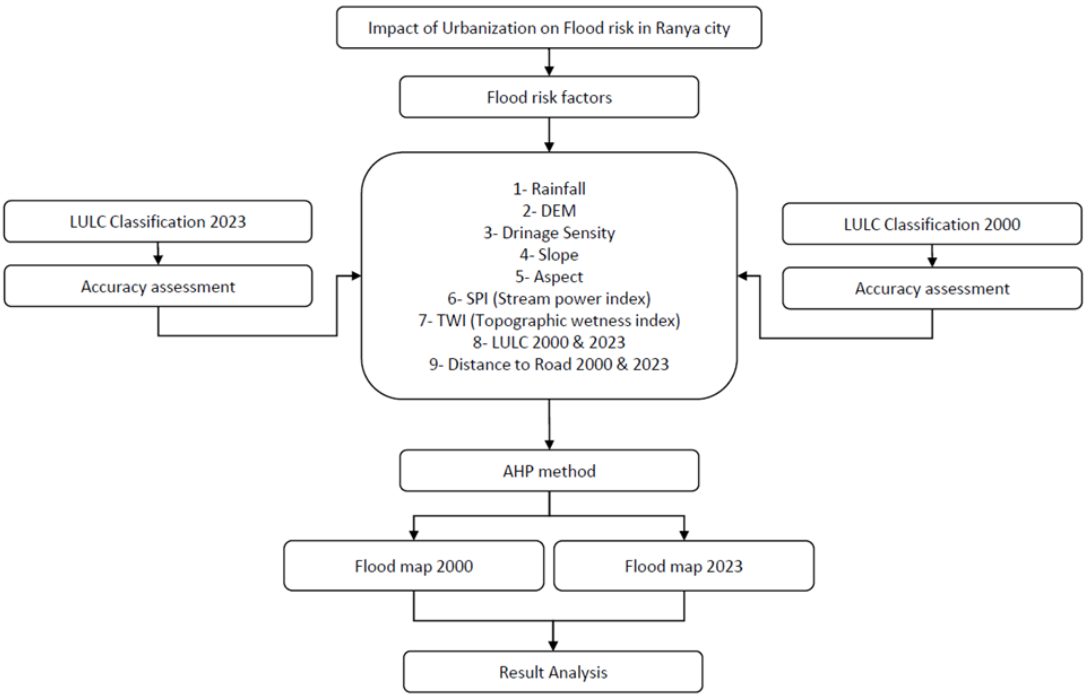

Figure 4: The methodology of the research.

Table 2: Pairwise comparison matrix for flood risk factors.

Factors	Rainfall	Drainage Density	Elevation	Slope	LULC	Aspect	TWI	SPI	Distance to Road
Rainfall	1.00	0.25	1.00	0.50	1.00	1.50	0.50	1.50	0.50
Drainage Density	2.00	1.00	2.00	2.00	2.00	2.00	2.00	2.00	0.50
Elevation	1.00	0.50	1.00	1.00	1.00	1.00	1.00	1.00	0.50
Slope	2.00	0.50	1.00	1.00	1.50	1.50	1.50	1.50	0.50
LULC	1.00	0.50	1.00	0.67	1.00	1.50	1.50	1.50	0.50
Aspect	0.67	0.50	1.00	0.67	0.67	1.00	1.00	1.00	0.33
TWI	2.00	0.50	1.00	0.67	0.67	1.00	1.00	2.00	0.50
SPI	0.67	0.50	1.00	0.67	0.67	1.00	1.00	1.00	0.50
Distance to Road	2.00	2.00	2.00	1.00	2.00	3.00	3.00	2.00	1.00

3.2 The Influences of Urban growth on Flooding

The present research utilised the AHP method with GIS to investigate the effects of urbanisation on the risk of flooding for the years 2000 and 2023. Taking into account the nine factors, the AHP method generated flood risk maps for the years 2000 and 2023 (Fig. 3). Four categories of flood risk have been identified (low, moderate, high and very high). In the year 2000, the area of flood hazard in the low hazard category was 22.5 km2 (84.4%), and in the very high hazard category was 0.23 km2 (0.9%). In addition, for the year 2023, 3.2 km2 was found to be in the low-hazard category, and 0.6 km2 was found to be in the very high-hazard category. When comparing 2023 to 2000, we see a 1.9% rise in very vulnerable regions and an 11.4% decline in low-hazard zones that were at risk of flooding (Table 4). High-risk flood zones tend to be in densely populated areas, especially in the city center. Low-risk flood zones, on the other hand, tend to be on barren land. The results demonstrated that the number of sites at very high risk of flooding has increased substantially because of road construction and new settlements. Identification of flood-prone zones during wet seasons is valuable for preventing floods, specifically in susceptible areas.

During heavy rainstorms, the water flowing into the sewers can exceed their capacity. This can cause sewers to become overloaded, resulting in flooding. Inadequate drainage channel design, poor maintenance of drainage infrastructure, and obstruction by waste carried by flood waters are additional causes of floods [47]. These wastes can block the flow of water through the sewer lines, causing it to back up and flood streets and homes. The flood protection system may reduce flood-related hazards and save individuals and assets in flood-prone areas [78]. In response to these flood incidents, local governments could implemented flood mitigation measures such as improving drainage systems and constructing new flood protection structures. However, given the unpredictability of weather patterns, fully preventing floods in Ranya and other parts of Iraq's Kurdistan Region remains a challenge. In addition, to reduce the impact of sewerage problems on flooding, it is recommended to implement measures such as regular sewer system maintenance and cleaning sewerage lines regularly, especially before rainy seasons. Furthermore, public education campaigns that inform the public about proper waste disposal methods can help to prevent blockages. Government entities and decision-makers can use the hazard analysis method outlined in this research, along with its results for vulnerable flood zones in Ranya, as a guide to improve emergency preparedness and strategic planning.

Table 3: Ranking and weight of each flood risk factors.

Factors	Class	Weight (%)	ranking	Factors	Class	Weight (%)	ranking
Elevation	533 to 569	8	1	Slope	0 to 2	12	5
	570 to 602		2		2to 5		4
	603 to 649		3		5 to 8		3
	650 to 720		4		8 to 15		2
	721 to 861		5		>30		0
Distance to Road (m)	<30	19	5	LULC	Built-up area	10	5
	30 to 60		4		Vegetation		2
	60 to 90		3		Barren land		1
	90 to 150		2	SPI	0.000000556 to 0.000001	8	1
	>2930		1		0.000001001 to 0.00001		2
TWI	-6.84 to -3.87	10	1		0.000010001 to 0.0001		3
	-3.87 to -2.57		2		0.000100001 to 0.001		4
	-2.57 to -0.127		3		0.001000001 to 0.020469133		5
	-0.127 to 1		4	Aspect	flat	7	5
	0 to 4.26		5		north		4
Drainage Density	4.26 to 400	17	5		northeast		3
	400 to 900		5		east		1
	900 to 1400		5		southeast		1
	1400 to 1700		2		south		1
	>1911		1		southwest		1
Rainfall	540 to 560	8	1		west		1
	560 to 570		2		northwest		3
	570 to 580		3		north		4
	580 to 590		4				
	590 to 606		5				

Table 4: The flood risk areas and percentages of Ranya city for 2000 and 2023.

	2000		2023		2000 – 2023	
Risk	Area (km^2)	%	Area (km^2)	%	Area (km^2)	%
Low	22.5	84.4	19.3	73	- 3.2	- 11.4
Moderate	2.74	11.2	4.32	16.4	+ 1.58	+ 5.2
High	0.97	3.5	2.21	8.4	+ 1.24	+ 4.9
Very high	0.23	0.9	0.6	2.2	+ 0.23	+ 1.9

4. Conclusions

Variations in LULC and immediate urban development contributed to an increase of floods in Ranya city due to demographic shifts and urban development. The primary purpose of this study was to evaluate the effect of urbanisation on floods over 23 years by looking at 9 key factors related to floods. Flood hazard maps for the years 2000 and 2023 were generated and analysed using AHP, GIS, and satellite remote sensing data. Based on classified LULC maps, between 2000 and 2023, built-up area and agriculture increased by about 25% and 9.6%, respectively, while open spaces decreased by 34.8%. The annual increase in built-up area was very high (1.09%), which played a central role in increasing the high vulnerable areas of flood in Ranya. The MCDM approach and a GIS were used to categorise flood risk maps (low, moderate, high and very high). According to the findings, compared to the year 2000, the potential flood areas increased by 1.9% in very highly vulnerable regions in 2023, while reduced by 11.4% in low vulnerable areas. Furthermore, the majority of places with a very high chance of flooding are in urban areas, particularly in city centres. Over 23 years in Ranya, road construction and new settlements have immensely raised the total areas in Ranya that are at high risk of flooding. The resulting flood hazard maps can be used to effectively mitigate damage in flood-prone areas of Ranya City. The method employed by this study allows researchers to efficiently monitor the urban environment. It also helps policymakers and government officials understand how urban development affects ecosystems.

5. Author's Contribution

The author contributed to the study conception and analysis were performed by [Kaifi Chomani]. The first draft of the manuscript was written and revised by [Kaifi Chomani]. The author read and approved the final manuscript.

6. Conflict of interest

The author declares that he has no conflict of interest.

References

[1] Khosravi K, Shahabi H, Pham BT, Adamowski J, Shirzadi A, Pradhan B, et al. A comparative assessment of flood susceptibility modeling using multi-criteria decision-making analysis and machine learning methods. Journal of Hydrology. 2019; 573: 311-23. https://doi.org/10.1016/j.jhydrol.2019.03.073.

[2] Malik S, Pal SC, Chowdhuri I, Chakrabortty R, Roy P, Das B. Prediction of highly flood prone areas by GIS based heuristic and statistical model in a monsoon dominated region of Bengal Basin. Remote Sensing Applications: Society and Environment. 2020; 19: 100343. https://doi.org/10.1016/j.rsase.2020.100343.

[3] Markantonis V, Meyer V, Lienhoop N. Evaluation of the environmental impacts of extreme floods in the Evros River basin using Contingent Valuation Method. Natural hazards. 2013; 69: 1535-49. https://doi.org/10.1007/s11069-013-0762-3.

[4] Borzi G, Roig A, Tanjal C, Santucci L, Tejada Tejada M, Carol E. Flood hazard assessment in large plain basins with a scarce slope in the Pampean Plain, Argentina. Environmental Monitoring and Assessment. 2021; 193: 1-14. https://doi.org/10.1007/s10661-021-08988-1.

[5] Malik S, Pal SC, Arabameri A, Chowdhuri I, Saha A, Chakrabortty R, et al. GIS-based statistical model for the prediction of flood hazard susceptibility. Environment, Development and Sustainability. 2021; 23: 16713-43. https://doi.org/10.1007/s10668-021-01377-1.

[6] Samanta RK, Bhunia GS, Shit PK, Pourghasemi HR. Flood susceptibility mapping using geospatial frequency ratio technique: a case study of Subarnarekha River Basin, India. Modeling Earth Systems and Environment. 2018; 4: 395-408. https://doi.org/10.1007/s40808-018-0427-z.

[7] Aryal D, Wang L, Adhikari TR, Zhou J, Li X, Shrestha M, et al. A model-based flood hazard mapping on the southern slope of Himalaya. Water. 2020;12(2):540. https://doi.org/10.3390/w12020540.
[8] Prama M, Omran A, Schröder D, Abouelmagd A. Vulnerability assessment of flash floods in Wadi Dahab Basin, Egypt. Environmental Earth Sciences. 2020; 79: 1-17. https://doi.org/10.1007/s12665-020-8860-5.
[9] Petrucci O, Aceto L, Bianchi C, Bigot V, Brázdil R, Pereira S, et al. Flood fatalities in Europe, 1980–2018: Variability, features, and lessons to learn. Water. 2019;11(8):1682. https://doi.org/10.3390/w11081682.
[10] Wang X, Xia J, Dong B, Zhou M, Deng S. Spatiotemporal distribution of flood disasters in Asia and influencing factors in 1980–2019. Natural Hazards. 2021;108(3):2721-38. https://doi.org/10.1007/s11069-021-04798-3.
[11] Hajat S, Ebi KL, Kovats S, Menne B, Edwards S, Haines A. The human health consequences of flooding in Europe and the implications for public health: a review of the evidence. Applied Environmental Science and Public Health. 2003; 1: 13-21.
[12] Christensen JH, Christensen OB. Severe summertime flooding in Europe. Nature. 2003;421(6925):805-6. https://doi.org/10.1038/421805a.
[13] Costache R, Arabameri A, Blaschke T, Pham QB, Pham BT, Pandey M, et al. Flash-flood potential mapping using deep learning, alternating decision trees and data provided by remote sensing sensors. Sensors. 2021;21(1):280. https://doi.org/10.3390/s21010280.
[14] Roy P, Pal SC, Chakrabortty R, Chowdhuri I, Malik S, Das B. Threats of climate and land use change on future flood susceptibility. Journal of Cleaner Production. 2020; 272: 122757. https://doi.org/10.1016/j.jclepro.2020.122757.
[15] Saha A, Pal SC, Arabameri A, Blaschke T, Panahi S, Chowdhuri I, et al. Flood susceptibility assessment using novel ensemble of hyperpipes and support vector regression algorithms. Water. 2021;13(2):241. https://doi.org/10.3390/w13020241.
[16] Takeuchi K, Chavoshian A, Simonovic SP. Floods: from risk to opportunity. J Flood Risk Manag. 2018; 11: e12046. https://doi.org/10.1111/jfr3.12046.
[17] Cred U. Economic Losses, Poverty & Disasters 1998-2017. Université Catholique de Louvain (UCL), Brussels, Belgium. 2018;33.
[18] Natarajan S, Radhakrishnan N. Flood hazard delineation in an ungauged catchment by coupling hydrologic and hydraulic models with geospatial techniques—A case study of Koraiyar basin, Tiruchirappalli City, Tamil Nadu, India. Environmental Monitoring and Assessment. 2020;192(11):689. https://doi.org/10.1007/s10661-020-08650-2.
[19] UCAR. 2010 [Available from: https://www.meted.ucar.edu/.
[20] Sunkpho J, Ootamakorn C. Real-time flood monitoring and warning system. Songklanakarin Journal of Science & Technology. 2011;33(2).
[21] Minh PT, Tuyet BT, Thao TTT. Application of ensemble Kalman filter in WRF model to forecast rainfall on monsoon onset period in South Vietnam. Science of the Earth. 2018;40(4):367-94. https://doi.org/10.15625/0866-7187/40/4/13134.
[22] Malczewski J. GIS-based multicriteria decision analysis: a survey of the literature. International journal of geographical information science. 2006;20(7):703-26. https://doi.org/10.1080/13658810600661508.
[23] Rahmati O, Zeinivand H, Besharat M. Flood hazard zoning in Yasooj region, Iran, using GIS and multi-criteria decision analysis. Geomatics, Natural Hazards and Risk. 2016;7(3):1000-17. https://doi.org/10.1080/19475705.2015.1045043.
[24] Zope P, Eldho T, Jothiprakash V. Impacts of urbanization on flooding of a coastal urban catchment: a case study of Mumbai City, India. Natural Hazards. 2015; 75: 887-908. https://doi.org/10.1080/19475705.2015.1045043.
[25] Dewan AM, Yamaguchi Y. Land use and land cover change in Greater Dhaka, Bangladesh: Using remote sensing to promote sustainable urbanization. Applied geography. 2009;29(3):390-401. http://dx.doi.org/10.1016/j.apgeog.2008.12.005.
[26] Zope PE, Eldho TI, Jothiprakash V. Impacts of land use–land cover change and urbanization on flooding: A case study of Oshiwara River Basin in Mumbai, India. CATENA. 2016;145:142-54 DOI: https://doi.org/10.1016/j.catena.2016.06.009.

[27] USGS. 2023 [Available from: https://earthexplorer.usgs.gov/.
[28] Melesse AM, Shih S. Spatially distributed storm runoff depth estimation using Landsat images and GIS. Computers and Electronics in Agriculture. 2002;37(1-3):173-83. https://doi.org/10.1016/S0168-1699(02)00111-4.
[29] CCKP. 2023 [Available from: https://climateknowledgeportal.worldbank.org/.
[30] ThiknH. 2023 [Available from: https://thinkhazard.org/en/.
[31] Ahmed A, Al Maliki A, Hashim B, Alshamsi D, Arman H. Flood Susceptibility Mapping of the Northern Iraq Using Morphometric and Principal Component Analyses. 2023. https://doi.org/10.1038/s41598-023-39290-4.
[32] Suriya S, Mudgal B. Impact of urbanization on flooding: The Thirusoolam sub watershed–A case study. Journal of hydrology. 2012; 412: 210-9. https://doi.org/10.1016/j.jhydrol.2011.05.008.
[33] Milly PC, Betancourt J, Falkenmark M, Hirsch RM, Kundzewicz ZW, Lettenmaier DP, et al. Stationarity is dead: Whither water management? Science. 2008;319(5863):573-4. https://doi.org/10.1126/science.1151915.
[34] Dewan AM, Kumamoto T, Nishigaki M. Flood hazard delineation in greater Dhaka, Bangladesh using an integrated GIS and remote sensing approach. Geocarto International. 2006;21(2):33-8. https://doi.org/10.1080/10106040608542381.
[35] Qi H, Altinakar MS. A GIS-based decision support system for integrated flood management under uncertainty with two dimensional numerical simulations. Environmental Modelling & Software. 2011;26(6):817-21. https://doi.org/10.1016/j.envsoft.2010.11.006.
[36] Pramojanee P, Tanavud C, Yongchalermchai C, Navanugraha C, editors. An application of GIS for mapping of flood hazard and risk area in Nakorn Sri Thammarat Province, South of Thailand. Proceedings of International Conference on Geo-Information for Sustainable Management; 1997.
[37] Kourgialas NN, Karatzas GP. Flood management and a GIS modelling method to assess flood-hazard areas—a case study. Hydrological Sciences Journal–Journal des Sciences Hydrologiques. 2011;56(2):212-25. https://doi.org/10.1080/02626667.2011.555836.
[38] González-Arqueros ML, Mendoza ME, Bocco G, Castillo BS. Flood susceptibility in rural settlements in remote zones: The case of a mountainous basin in the Sierra-Costa region of Michoacán, Mexico. Journal of environmental management. 2018; 223: 685-93. https://doi.org/10.1016/j.jenvman.2018.06.075.
[39] Wheater H, Jakeman A, Beven K. Progress and directions in rainfall-runoff modelling. 1993.
[40] Bulti DT, Abebe BG. A review of flood modeling methods for urban pluvial flood application. Modeling earth systems and environment. 2020; 6: 1293-302. https://doi.org/10.1007/s40808-020-00803-z.
[41] Tehrany MS, Kumar L. The application of a Dempster–Shafer-based evidential belief function in flood susceptibility mapping and comparison with frequency ratio and logistic regression methods. Environmental earth sciences. 2018; 77: 1-24. https://doi.org/10.1007/s12665-018-7667-0.
[42] Falah F, Rahmati O, Rostami M, Ahmadisharaf E, Daliakopoulos IN, Pourghasemi HR. Artificial neural networks for flood susceptibility mapping in data-scarce urban areas. Spatial modeling in GIS and R for Earth and Environmental Sciences: Elsevier; 2019. p. 323-36. https://doi.org/10.1016/B978-0-12-815226-3.00014-4.
[43] Dodangeh E, Panahi M, Rezaie F, Lee S, Bui DT, Lee C-W, et al. Novel hybrid intelligence models for flood-susceptibility prediction: Meta optimization of the GMDH and SVR models with the genetic algorithm and harmony search. Journal of Hydrology. 2020; 590: 125423. https://doi.org/10.1016/j.jhydrol.2020.125423.
[44] Wang Y, Hong H, Chen W, Li S, Panahi M, Khosravi K, et al. Flood susceptibility mapping in Dingnan County (China) using adaptive neuro-fuzzy inference system with biogeography based optimization and imperialistic competitive algorithm. Journal of environmental management. 2019; 247: 712-29. https://doi.org/10.1016/j.jenvman.2019.06.102.
[45] Zhu G-N, Hu J, Qi J, Gu C-C, Peng Y-H. An integrated AHP and VIKOR for design concept evaluation based on rough number. Advanced Engineering Informatics. 2015;29(3):408-18. https://doi.org/10.1016/j.aei.2015.01.010.

[46] Qaiser K, Yuan Y, Lopez R. Urbanization impacts on flooding in the Kansas River Basin and evaluation of wetlands as a mitigation measure. Transactions of the ASABE. 2012;55(3):849-59.

[47] Sissakian VK, Al-Ansari N, Adamo N, Abdul Ahad ID, Abed SA. Flood Hazards in Erbil City Kurdistan Region Iraq, 2021: A Case Study. Engineering. 2022;14(12):591-601. https://doi.org/10.4236/eng.2022.1412044.

[48] Askar S, Zeraat Peyma S, Yousef MM, Prodanova NA, Muda I, Elsahabi M, et al. Flood Susceptibility Mapping Using Remote Sensing and Integration of Decision Table Classifier and Metaheuristic Algorithms. Water. 2022;14(19):3062. https://doi.org/10.3390/w14193062.

[49] Gigović L, Pamučar D, Božanić D, Ljubojević S. Application of the GIS-DANP-MABAC multi-criteria model for selecting the location of wind farms: A case study of Vojvodina, Serbia. Renewable energy. 2017; 103: 501-21. https://doi.org/10.1016/j.renene.2016.11.057.

[50] Zhong Q-b, Chen F. Trajectory planning for biped robot walking on uneven terrain–Taking stepping as an example. CAAI Transactions on intelligence technology. 2016;1(3):197-209. https://doi.org/10.1016/j.trit.2016.10.009.

[51] Gigović L, Pamučar D, Bajić Z, Milićević M. The combination of expert judgment and GIS-MAIRCA analysis for the selection of sites for ammunition depots. Sustainability. 2016;8(4):372. https://doi.org/10.3390/su8040372.

[52] Sowmya K, John C, Shrivasthava N. Urban flood vulnerability zoning of Cochin City, southwest coast of India, using remote sensing and GIS. Natural Hazards. 2015; 75: 1271-86.

[53] Wang Y, Li Z, Tang Z, Zeng G. A GIS-based spatial multi-criteria approach for flood risk assessment in the Dongting Lake Region, Hunan, Central China. Water resources management. 2011; 25: 3465-84. https://doi.org/10.1007/s11069-014-1372-4.

[54] Gerl T, Bochow M, Kreibich H. Flood damage modeling on the basis of urban structure mapping using high-resolution remote sensing data. Water. 2014;6(8):2367-93. https://doi.org/10.3390/w6082367.

[55] Chau VN, Holland J, Cassells S, Tuohy M. Using GIS to map impacts upon agriculture from extreme floods in Vietnam. Applied Geography. 2013; 41: 65-74. https://doi.org/10.1016/j.apgeog.2013.03.014.

[56] Kazakis N, Kougias I, Patsialis T. Assessment of flood hazard areas at a regional scale using an index-based approach and Analytical Hierarchy Process: Application in Rhodope–Evros region, Greece. Science of the Total Environment. 2015; 538: 555-63. https://doi.org/10.1016/j.scitotenv.2015.08.055.

[57] Papaioannou G, Vasiliades L, Loukas A. Multi-criteria analysis framework for potential flood prone areas mapping. Water resources management. 2015; 29: 399-418. https://doi.org/10.1007/s11269-014-0817-6.

[58] Meyer V, Scheuer S, Haase D. A multicriteria approach for flood risk mapping exemplified at the Mulde river, Germany. Natural hazards. 2009; 48: 17-39. https://doi.org/10.1007/s11069-008-9244-4.

[59] Gigović L, Pamučar D, Bajić Z, Drobnjak S. Application of GIS-interval rough AHP methodology for flood hazard mapping in urban areas. Water. 2017;9(6):360. https://doi.org/10.3390/w9060360.

[60] Fernández D, Lutz MA. Urban flood hazard zoning in Tucumán Province, Argentina, using GIS and multicriteria decision analysis. Engineering Geology. 2010;111(1-4):90-8. http://dx.doi.org/10.1016/j.enggeo.2009.12.006.

[61] Siddayao GP, Valdez SE, Fernandez PL. Analytic hierarchy process (AHP) in spatial modeling for floodplain risk assessment. International Journal of Machine Learning and Computing. 2014;4(5):450. https://doi.org/10.7763/IJMLC.2014.V4.453.

[62] Liu H, Tang H, Xiao W, Guo Z, Tian L, Gao Y. Sequential Bag-of-Words model for human action classification. CAAI Transactions on Intelligence Technology. 2016;1(2):125-36.

[63] Bathrellos G, Karymbalis E, Skilodimou H, Gaki-Papanastassiou K, Baltas E. Urban flood hazard assessment in the basin of Athens Metropolitan city, Greece. Environmental Earth Sciences. 2016; 75: 1-14. https://doi.org/10.1007/s12665-015-5157-1.

[64] Liu H, Wang C, Gao Y. Scene-adaptive hierarchical data association and depth-invariant part-based appearance model for indoor multiple objects tracking. CAAI Transactions on Intelligence Technology. 2016;1(3):210-24.
[65] GKSAT. 2023 [Available from: https://www.gksat.tv/.
[66] KTV. 2023 [Available from: https://kurdistantv.net/.
[67] KPD. 2023 [Available from: https://www.kurdipedia.org/.
[68] PUK. 2023 [Available from: https://www.pukmedia.com/.
[69] XENDAN. 2023 [Available from: https://www.xendan.org/.
[70] K24. 2023 [Available from: https://www.kurdistan24.net/en.
[71] Gaznayee HAA, Al-Quraishi AMF, Mahdi K, Messina JP, Zaki SH, Razvanchy HAS, et al. Drought Severity and Frequency Analysis Aided by Spectral and Meteorological Indices in the Kurdistan Region of Iraq. Water. 2022;14(19):3024. https://doi.org/10.3390/w14193024.
[72] Mustafa N. ARIDITY INDEX BASED ON TEMPERATURE AND RAINFALL DATA FOR KURDISTAN REGION-IRAQ. The Journal of The University of Duhok. 2018; 21: 65-80. https://doi.org/10.26682/sjuod.2018.21.1.6.
[73] Ghosh A, Kar SK. Application of analytical hierarchy process (AHP) for flood risk assessment: a case study in Malda district of West Bengal, India. Natural Hazards. 2018; 94: 349-68. https://doi.org/10.1007/s11069-018-3392-y.
[74] Allafta H, Opp C. GIS-based multi-criteria analysis for flood prone areas mapping in the trans-boundary Shatt Al-Arab basin, Iraq-Iran. Geomatics, Natural Hazards and Risk. 2021;12(1):2087-116. https://doi.org/10.1080/19475705.2021.1955755.
[75] Aydin MC, Sevgi Birincioğlu E. Flood risk analysis using gis-based analytical hierarchy process: a case study of Bitlis Province. Applied Water Science. 2022;12(6):122. https://doi.org/10.1007/s13201-022-01655-x.
[76] ESRI. 2023 [Available from: https://www.esri.com/.
[77] Termeh SVR, Kornejady A, Pourghasemi HR, Keesstra S. Flood susceptibility mapping using novel ensembles of adaptive neuro fuzzy inference system and metaheuristic algorithms. Science of the Total Environment. 2018; 615: 438-51. https://doi.org/10.1016/j.scitotenv.2017.09.262.
[78] Khan SI, Hong Y, Wang J, Yilmaz KK, Gourley JJ, Adler RF, et al. Satellite remote sensing and hydrologic modeling for flood inundation mapping in Lake Victoria basin: Implications for hydrologic prediction in ungauged basins. IEEE Transactions on Geoscience and Remote Sensing. 2010;49(1):85-95. https://doi.org/10.1109/TGRS.2010.2057513.